

Special Article - Radiology Imaging

Reliability of Evaluation of the Craniocervical Junction by XR, CT and MRI in Patients with Genetic Skeletal Diseases

Cunha Júnior AL^{1*}, Silva Champs AP², Meirelles Mello C¹, Barduco Carvalho CM³, Carvalho Godinho FJ³, Machado Navarro MM³ and Abreu Ferrari TC⁴

¹Department of Radiology and Diagnostic Imaging, Rede SARAH de Hospitais de Reabilitação, Brazil

²Department of Spinal Injury Rehabilitation, Rede SARAH de Hospitais de Reabilitação, Brazil

³Department of Pediatrics, Rede SARAH de Hospitais de Reabilitação, Brazil

⁴Department of Clinical Medicine, Universidade Federal de Minas Gerais, Brazil

*Corresponding author: Antônio Lopes Cunha Júnior, Department of Radiology and Diagnostic Imaging, Rede SARAH de Hospitais de Reabilitação, Av. Amazonas, 5953. Gameleira, 30510-000. Belo Horizonte, MG, Brazil

Received: December 07, 2020; Accepted: December 30, 2020; Published: January 06, 2021

Abstract

Background: Craniocervical Junction (CCJ) imaging interpretation in patients with Genetic Skeletal Disorders (GSDs) is challenging due to bone tissue disorganization. CCJ abnormalities and spinal cord compression present potential risks.

Purpose: To describe and compare CCJ measurements in patients with GSDs using XR, CT and MRI.

Materials and Methods: This cross-sectional observational and analytical study prospectively included 287 participants. Clinical evaluation, spine XR, CCJ dynamic CT, and brain and spinal cord MRI data were recorded. The participants were separated into groups with and without cervical Spinal Cord Injury (cSCI). Three craniometry measurements were performed with each imaging method, and the reliability and reproducibility were analyzed.

Results: cSCI was identified in 4.5%. Spinal canal stenosis at C2 (78.8%), a narrowed foramen magnum (12.5%), os odontoideum (5.9%), ventral cervicomedullary encroachment by the odontoid (20.2%), and basilar impression/invagination (12.9%) were associated with an increased chance of cSCI. CT showed the highest accuracy for bone abnormality diagnoses. The cutoff points for the spinal canal to diagnose cSCI were 17.3 mm with XR, 12.9 mm with CT and 10.4 mm with MRI.

Conclusion: CT showed good reliability and reproducibility in evaluating the CCJ in GSDs. XR presented more limitations but provided complementary data to MRI.

Keywords: Spinal cord injury; Spinal cord compression; Imaging; Interobserver reliability; Intraobserver reproducibility

Abbreviations

CCJ: Craniocervical Junction; cSCI: cervical Spinal Cord Injury; GSD(s): Genetic Skeletal Disorder(s)

Introduction

Evaluation of the Craniocervical Junction (CCJ) by imaging methods is a diagnostic challenge: it can be performed by different methods, involves several measures and allows identification of several alterations such as platybasia [1], clivus hypoplasia [2], a narrowed foramen magnum [3], basilar impression/invagination [1], atlantoaxial instability [4], spinal canal stenosis at C2 [5], cervicomedullary encroachment by the odontoid [6], basio-occipital hypoplasia [6] and atlanto-occipital instability [7,8].

Several types of Genetic Skeletal Disorders (GSDs) exist, which are rare diseases in isolation, but as a group, they affect a significant number of patients [9] at risk for neurological complications [10,11]. In GSDs, CCJ abnormalities are relatively common, and imaging interpretation is more difficult due to disorganization of bone tissue [8,10]. Currently, patients with GSDs are treated by different medical specialties due to increased life expectancy [9].

Prevention of compressive Spinal Cord Injury (SCI) is a priority in patients with GSDs, especially due to the severity and irreversibility of lesions [12]. In addition, these patients may have primary neurological manifestations of the disease itself [13] and orthopedic complications with bone and joint deformities [14] that impair neurological examination, which provides important information for interpreting structural abnormalities of the CCJ [15]. Urological complications due to SCI, such as neurogenic bladder and reflux nephropathy, are also serious and costly [16]. Despite important technological advances, the benefits and risks of foramen magnum or spinal canal surgical decompression and atlantoaxial or atlanto-occipital joint fixation remain controversial in cases of spinal instability [17-19]. In this context, scientific knowledge generated in specialized centers regarding the care and treatment of patients with GSDs may be very useful.

This study aimed to describe and compare CCJ imaging findings on digital Radiography (XR), CT and MRI in the diagnosis of platybasia, clivus hypoplasia, a narrowed foramen magnum, basilar impression/invagination, atlantoaxial instability, spinal canal stenosis at C2, cervicomedullary encroachment by the odontoid, basio-

occipital hypoplasia and atlanto-occipital instability, which can cause spinal cord compression or injury.

Materials and Methods

Editorial policies and ethical considerations

The project protocol was approved by the institution's Ethics Committee (CAAE 49433215.5.0000.0022). Patients and/or their legal guardians who agreed to participate signed an informed consent form.

Study design

This cross-sectional observational study with the prospective inclusion of the participants was performed at the Rehabilitation Hospital from 2001 to 2016.

Patients

The medical records of patients with congenital bone changes, orthopedic deformities and/or a demand for rehabilitation were reviewed, and those with a definitive diagnosis of GSD and an age \geq four years were enrolled. We excluded patients who refused to participate, could not undergo all imaging modalities, were lost to medical follow-up or had severe mental retardation. All participants underwent medical consultations, imaging examinations and laboratory tests on the same day. The participants were separated into two groups: one with and another without cSCI. Patients with neurological abnormalities unrelated to GSDs were excluded from the analysis. The sample size was estimated based on 456 patients with a definitive diagnosis of GSD, a proportion of 4.5% for those with cSCI, a permissible error of 0.05, and a 95% confidence level, resulting in 58 patients.

Image acquisition and analysis

Previous radiologic studies, an analysis of medical records and a geneticist evaluation allowed the patients to be grouped according to the Classification and Nosology of the International Society for Skeletal Dysplasia [20]. Clinical manifestations of brain, spinal cord and peripheral nerve injuries were investigated by a physiatrist. SCI was classified according to the International Standards for Neurological Classification of Spinal Cord Injuries, revision 2019 [15].

The following imaging examinations were performed: cervical spine XR in the lateral view on an Axiom Luminous dRF device (Siemens, Germany); brain and spinal cord MRI on a 1.5T Optima MR450w device (General Electric, United States) with 3D-weighted T1 (TR: 500 msec/TE: 42 msec), sagittal and axial FAST SPIN ECHO T2-weighted (TR: 3290 msec/TE: 120 msec) and cerebrospinal fluid flow sequences (TR: 27 msec); and dynamic CCJ CT on a 16-row multidetector CT scanner Bright Speed (General Electric, United States). Sub-millimeter spatial resolution images without contrast were acquired and reconstructed in 0.625-mm thick and spaced slices.

A systematic evaluation of the CCJ imaging examinations was carried out by two observers and by one observer at two different time points without knowledge of the previous results. MRI measurements were obtained using T2-weighted sequences. The atlanto-occipital joint axis angle was measured only on CT. The foramen magnum latero-lateral diameter, atlanto-occipital interval and cervicomedullary encroachment by the odontoid were measured

on CT and MRI. The other CCJ measurements were performed on XR, CT and MRI.

Craniometry was used to diagnose changes in the CCJ based on the following defined criteria: platybasia if the basal angle was $> 150^\circ$ [1], clivus hypoplasia if the clivus length was < 37.7 mm [6], a narrowed foramen magnum if the anteroposterior diameter was < 28.5 mm and/or the latero-lateral diameter was < 23 mm [6], basilar impression/invagination if the distance from the apex of the odontoid above the Chamberlain line was > 5 mm and/or the distance from the McGregor line was > 7 mm [1], atlantoaxial instability if the atlantodental interval was > 3 mm in a neutral position [4,6,8], spinal canal stenosis at C2 if the anteroposterior diameter of the spinal canal was < 19 mm [21], ventral cervicomedullary encroachment by the odontoid if the encroachment was > 8.7 mm [6], basio-occipital hypoplasia if the atlanto-occipital joint axis angle was $> 127^\circ$ [6] and atlanto-occipital instability if at least two parameters were abnormal: a basion-dens interval > 9 mm, and/or a basion-axial interval > 12 mm, and/or a powers ratio > 0.9 and/or an atlanto-occipital interval > 1.4 mm [4,7,8,22].

Statistical analysis

The statistical software R (R Core Team, Vienna, Austria) was used for all analyses.

Observer measurements of each CCJ parameter were compared to assess reproducibility.

Reliability was analyzed by the percentage of agreement according to the Bland-Altman method for quantitative variables, and CT was considered the gold standard for comparison.

The parameter measurements were also categorized as normal or abnormal based on predefined reference values according to a literature review, and the kappa index was used to compare nominal variables. A kappa value less than zero indicated disagreement, 0.01 to 0.20 indicated that the agreement was achieved by chance, 0.21 to 0.40 indicated fair agreement, 0.41 to 0.60 indicated moderate agreement, 0.61 to 0.80 indicated substantial agreement, and 0.81 to 1.00 indicated nearly perfect agreement [23].

A Receiver Operating Characteristic (ROC) curve was used to obtain cutoff points for the anteroposterior diameter of the spinal canal at C2 on XR, CT and MRI for the diagnosis of spinal canal stenosis associated with cSCI in patients with GSDs. The areas under the curve were compared between the imaging methods.

Results

Participant demographics

From an initial population of 685 patients, after reviewing medical records, 456 patients were selected. The flow chart of the study is provided in Figure 1. The sample consisted of 287 participants with 41 disorders in 23 different GSD groups. The most frequent GSD groups according to the Classification and Nosology of the International Society of Skeletal Dysplasia [20] were as follows: abnormal mineralization (24.4%), disorganized development of skeletal components (17.0%), osteogenesis imperfecta and decreased bone density (13.6%), spondylo-epi-(meta)-physeal dysplasias (8.0%), multiple epiphyseal dysplasias and pseudoachondroplasia (7.7%), fibroblast growth factor receptor 3 chondrodysplasias (7.0%),

Table 1: Demographics of the Study Participants.

Demographics	Number of patients (n = 287)
Median age (IQR)	22 years (15-32 years)
Women	153/287 (53.0%)
cSCI	13/287 (4.5%)
Stature (IQR)	145 cm (131-157 cm)
Weight	59 Kg (39-63 Kg)
Trunk length (IQR)	47 cm (42-51 cm)
Occipitofrontal circumference (IQR)	56 cm (50-65 cm)
Upper segment length (IQR)	71 cm (69-77 cm)
Lower segment length (IQR)	77 cm (69-86 cm)
Wingspan (IQR)	147 cm (131-161 cm)
Body mass index (IQR)	24 (20-29)
Joint deformity	216/287 (75.3%)
Lower limb discrepancy	123/287 (42.9%)
Low back pain	120/287 (41.8%)
Headache	99/287 (34.5%)
Ligament laxity	46/287 (16.0%)
Abnormal neuropsychomotor development	31/287 (10.8%)
Joint dislocation	19/287 (6.6%)

IQR: Interquartile Range; SCI: Spinal Cord Injury

metaphyseal dysplasias (4.2%), spondylometaphyseal dysplasias (3.8%) and lysosomal storage diseases with skeletal involvement ([dysostosis multiplex] 3.2%). The classes of SCI were as follows: C in eight (2.8%) patients, D in 24 (8.4%) patients, and * in 41 (14.3%) individuals. In 15 (5.2%) of the patients classified as having class 'SCI, common fibular nerve injuries related to orthopedic deformities (genu varus and genu valgus) and/or sequelae of surgical treatment were detected in the clinical examination. Spinal Cord Injury

Without Radiographic Abnormality (SCIWORA) was found in 25 (8.7%) patients.

The demographics of the participants are presented in Table 1. One hundred fifty-three patients (53%) were woman. The patients' ages ranged from five to 70 years, with a median of 22 (Interquartile Range [IQR]: 15-32) years, an asymmetric distribution, and a larger number of patients in the second and third decades of life.

CCJ Abnormalities

CSCI was noted in 13/287 (4.5%) individuals, including patients with C2 canal stenosis, a narrowed foramen magnum, os odontoideum, platybasia, cervicomedullary encroachment by the odontoid, basilar impression/invagination, atlanto-occipital instability, basio-occipital hypoplasia and atlantoaxial instability. No cSCI was noted in patients with a terminal bone.

The CCJ findings are listed in Table 2. A higher chance of cSCI was noted in the presence of spinal canal stenosis, a narrow foramen magnum, os odontoideum, cervicomedullary encroachment by the odontoid and basilar impression/invagination. Platybasia, basio-occipital hypoplasia, atlantoaxial instability, atlanto-occipital instability and a terminal bone at C2 were not associated with a higher chance of cSCI in this sample.

Interobserver reproducibility

CT showed better interobserver reproducibility for CCJ parameter measurements than XR and MRI (Figures 2 and 3 and Tables S1 and S2).

Imaging method agreement

The percentage of concordant measurements obtained on XR, CT and MRI based on numerical values compared using the Bland-Altman method was generally superior to that based on the dichotomous (normal or abnormal) analysis performed using kappa

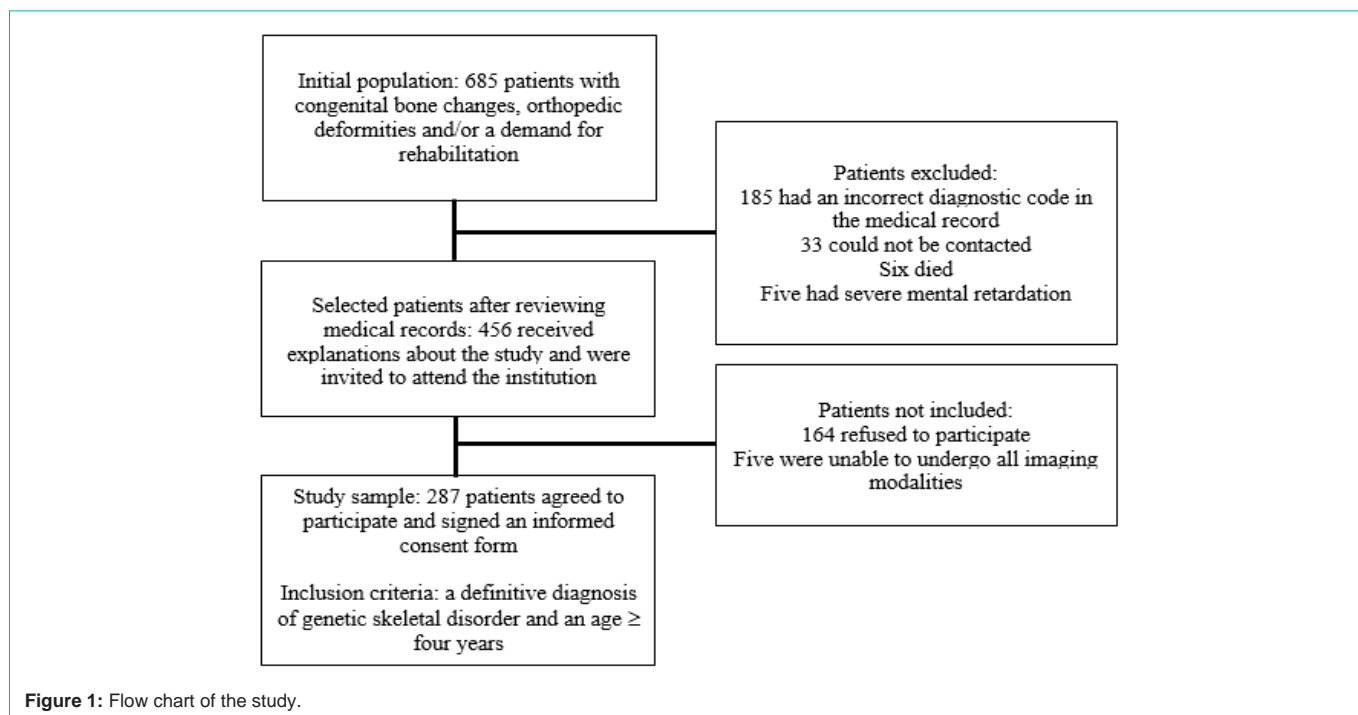


Figure 1: Flow chart of the study.

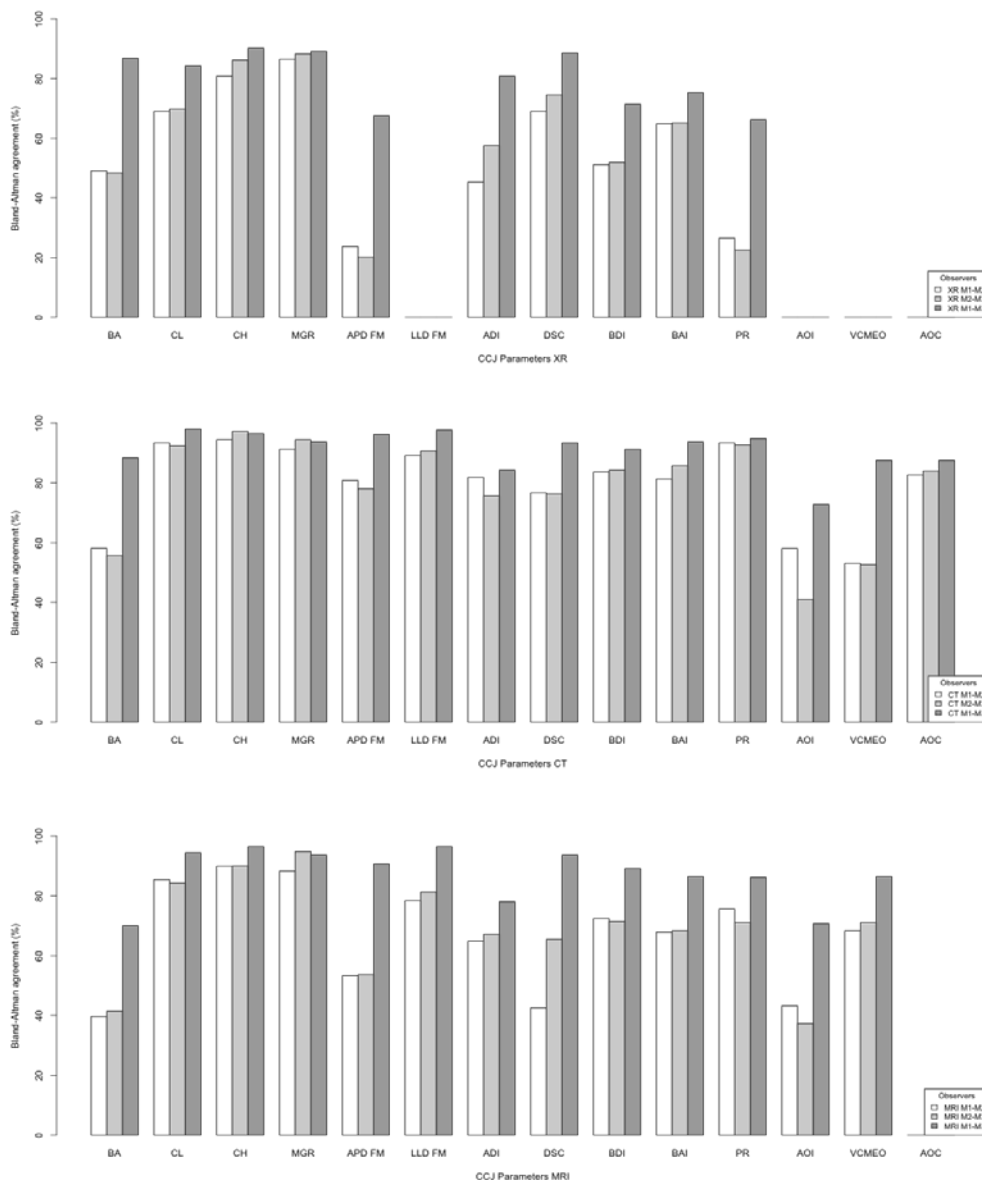


Figure 2: CCJ measurement reliability and reproducibility on XR (a), CT (b) and MRI (c) by the Bland-Altman method. M1: First Observer's Measurement 1; M2: Second Observer's Measurement; M3: First Observer's Measurement 2; CCJ: Craniocervical Junction; BA: Basal Angle; CL: Clivus Length; CH: distance from the tip of the odontoid process to the Chamberlain Line; MGR: distance from the tip of the odontoid process to the McGregor line; APD: Anteroposterior Diameter; FM: Foramen Magnum; LLD: Latero-Lateral Diameter; ADI: Atlantodental Interval; DSC: Anteroposterior Diameter of the Spinal Canal; BDI: Basion-Dens Interval; BAI: Basion-Axial Interval; PR: Powers Ratio; AOI: Atlanto-Occipital Interval; VCME0: Ventral Cervicomedullary Encroachment by the Odontoid; AOC: Atlanto-Occipital Joint Axis Angle.

statistics, as shown in Figure 4 and Table S3. A high correlation was observed between MRI and CT measurements of the CCJ parameters, as shown in Table 3.

Measurements of the basal angle and the distance from the tip of the odontoid process to the Chamberlain line and to the McGregor line on XR were concordant and correlated with the same parameters measured on CT. The agreement and correlation for the measurements of these parameters between XR and CT were lower than those between MRI and CT.

The measurements of the anteroposterior diameter of the spinal

canal at C2 and clivus length on XR were higher than those on CT, with less agreement and a higher determination coefficient in relation to the other parameter measurements of the CCJ, indicating constant bias, as shown in Figure S1a and b and Figure 5a and b. The measurements of the anteroposterior diameter of the spinal canal at C2 on MRI were lower than those on CT, as shown in Figure 5c and d.

The atlantodental interval, basio dental interval and atlanto-occipital interval measured by MRI had the lowest correlations with the measurements of these parameters on CT, as shown in Table 3. On MRI and CT, when the measurements of the atlantodental interval were greater than 2.0 mm, as shown in Figure 6a and b), and those of

Table 2: CCJ Abnormalities in Patients with GSDs with and without cSCI.

CCJ abnormality	n (%)	CSCI (%)	No cSCI (%)	p-value*	OR (95% CI)
Spinal canal stenosis at C2	226/287 (78.8)	13/226 (5.8)	213/226 (94.2)	<.01	∞ (∞-10.2)
Narrowed foramen magnum	36/287 (12.5)	7/36 (19.4)	29/36 (80.6)	<.01	9.7 (2.6-37.6)
Os odontoideum	17/287 (5.9)	4/17 (23.5)	13/17 (76.5)	<.01	8.8 (1.7-37.1)
VCMEO	58/287 (20.2%)	7/58 (12.1)	51/58 (87.9)	<.01	5.1 (1.4-19.1)
Basilar impression/ invagination	37/287 (12.9%)	5/37 (13.5)	32/37 (86.5)	<.01	4.7 (1.1-17.4)
Platybasia	5/287 (1.7%)	1/5 (20.0)	4/5 (80.0)	.21	5.6 (0.1-62.3)
Basio-occipital hypoplasia	168/287 (58.5%)	10/168 (6.0)	158/168 (94.0)	.34	1.8 (0.5-7.9)
Atlanto-occipital instability	9/287 (3.1%)	1/9 (11.1)	8/9 (88.9)	.35	2.8 (0.1-23.7)
Atlantoaxial instability	20/287 (7.0%)	1/20 (5.0)	19/20 (95.0)	1.00	1.1 (0.1-8.4)
Terminal bone	6/287 (2.1%)	0/6 (0.0)	6/6 (100.0)	1.00	0.0 (0-19.4)

CCJ: Craniocervical Junction; GSD: Genetic Skeletal Disorder; SCI: Cervical Spinal Cord Injury; *X² or Fisher's exact test; OR: Odds Ratio; CI: Confidence Interval; VCMEO: Ventral Cervicomedullary Encroachment by the Odontoid

Table 3: Correlations of the CCJ Parameters Assessed by XR, CT and MRI.

CCJ parameter	RX-CT (rho)	r ²	p*	MRI-CT (rho)	r ²	p*
DSC	.82	66%	<.01	.85	72%	<.01
Clivus length	.80	64%	<.01	.93	86%	<.01
Basal angle	.79	63%	<.01	.87	76%	<.01
MGR	.69	36%	<.01	.78	60%	<.01
CH	.68	46%	<.01	.80	64%	<.01
Basion-axial interval	.62	39%	<.01	.73	54%	<.01
Atlantodental interval	.56	31%	<.01	.48	23%	<.01
Anteroposterior diameter FM	.33	11%	<.01	.70	48%	<.01
Powers ratio	.26	7%	<.01	.81	65%	<.01
Basion-dens interval	.23	5%	<.01	.51	26%	<.01
Latero-lateral diameter FM	-	-	-	.87	75%	<.01
VCMEO	-	-	-	.76	58%	<.01
Atlanto-occipital interval	-	-	-	.39	15%	<.01

CCJ: Craniocervical Junction; r²: Coefficient of Determination; *Spearman's test; DSC: Anteroposterior Diameter of the Spinal Canal at C2; MGR: Distance from the tip of the odontoid process to the McGregor line; CH: Distance from the tip of the odontoid process to the Chamberlain line; FM: foramen magnum; VCMEO: Ventral Cervicomedullary Encroachment by the Odontoid.

the atlanto-occipital interval were greater than 2.3 mm, disagreement between the measurements was noted, as shown in Figure 6c and d. The powers ratio measurements on XR and CT showed less agreement and weaker correlations compared to the powers ratio measurements between MRI and CT, as shown in Figure S2.

Anteroposterior diameter of the spinal canal at C2

The ROC curve provided different cutoff points for the anteroposterior diameter of the spinal canal at C2 on XR, CT and

Table 4: Anteroposterior Diameter of the Spinal Canal at C2 (DSC) on XR, CT and MRI for the Diagnosis of cSCI.

DSC	AUC (95% CI)	p*	Cutoff	Se% (95% CI)	Sp% (95% CI)
XR	0.73 (0.57; 0.99)	<.01	17.3 mm	92 (82, 100)	57 (46, 68)
CT	0.75 (0.61; 0.89)	<.01	12.9 mm	96 (88, 100)	50 (39, 61)
MRI	0.84 (0.72; 0.97)	<.01	10.4 mm	99 (95, 100)	64 (54, 75)

DSC: Anteroposterior Diameter of the Spinal Canal at C2; SCI: Spinal Cord Injury; AUC: Area Under the ROC Curve; CI: Confidence Interval; *X² or Fisher's exact test; Se: Sensitivity; Sp: Specificity.

MRI associated with cSCI, as shown in Table 4 and Figure S3.

Discussion

Imaging examinations allowed us to describe craniocervical junction bone abnormalities, assess the extent of spinal cord injury, and verify the association between these bone changes and neurological damage in a large sample of patients with different types of genetic skeletal disorders. Medical history, physical examination, XR, CT and MRI results were analyzed with a well-defined methodology and blind interpretation of the results. Reliability analysis showed that the agreement between the craniocervical junction parameters measured using different imaging methods, as well as the agreement for measurements between observers, varies, particularly depending on the craniocervical junction parameter evaluated.

cSCI occurred in a small number of patients, which is consistent with other studies [12,24,25]. Advances in scientific knowledge and greater accessibility to specialized medical care have increased the survival of patients with GSDs and the likelihood of neurological complications [12,13,24,26].

The more frequent CCJ abnormalities in patients with GSDs are spinal canal stenosis at C2 and basio-occipital hypoplasia, which are probably related to bone tissue disorganization, abnormal ossification and slower bone growth [10,11,24,27].

Spinal canal stenosis, a narrowed foramen magnum, os odontoideum, cervicomedullary encroachment by the odontoid and basilar impression/invagination were associated with an increased chance of cSCI in our patients with GSDs, which is consistent with previous studies [10,11,27-29]. Disproportion between the dimensions of the spinal cord and the diameter of the canal may exist and may cause direct spinal cord compression or microtrauma and ischemia due to vascular involvement [10,28,30,31].

The frequency of cervicomedullary encroachment by the odontoid on CT and MRI was higher than the number of patients with cSCI, suggesting that some degree of compression may exist without causing this injury. The clinical examination must be carefully performed. Neurological abnormalities may be also related to brain injury, orthopedic deformities, compressive myelopathy, thoracic and lumbar radiculopathy, peripheral nerve injuries and other causes of neurological injury unrelated to GSDs [15,27,29].

CT was the best method for defining bone anatomy and should be performed when surgical treatment is indicated and is recommended when atlanto-occipital instability is suspected [1,11,32].

Comparison of the reliability of craniometry by the imaging methods revealed that the measurements obtained showed greater agreement between the categories based on the dichotomous analysis

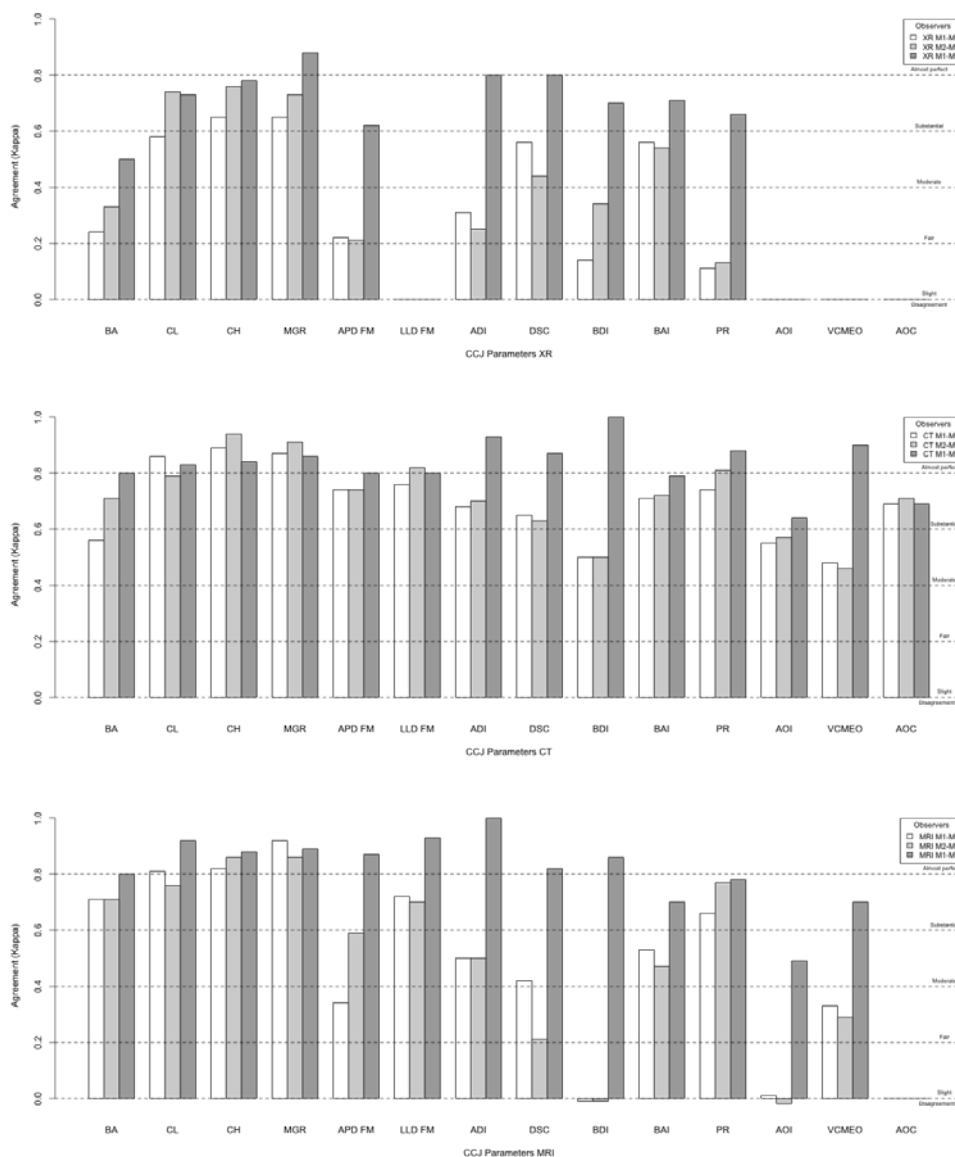


Figure 3: CCJ measurement reliability and reproducibility on XR (a), CT (b) and MRI (c) by kappa statistics. M1: First Observer's Measurement 1; M2: Second Observer's Measurement; M3: First Observer's Measurement 2; CCJ: Craniocervical Junction; BA: Basal Angle; CL: Clivus Length; CH: Distance from the tip of the odontoid process to the Chamberlain Line; MGR: Distance from the tip of the odontoid process to the McGregor line; APD: Anteroposterior Diameter; FM: Foramen Magnum; LLD: Latero-Lateral Diameter; ADI: Atlantodental Interval; DSC: Anteroposterior Diameter of the Spinal Canal; BDI: Basion-Dens Interval; BAI: Basion-Axial Interval; PR: Powers Ratio; AOI: Atlanto-Occipital Interval; VCME0: Ventral Cervicomedullary Encroachment by the Odontoid; AOC: Atlanto-Occipital Joint Axis.

(normal or abnormal); therefore, the reference values should be different according to the method. As good correlations for the CCJ parameters were identified between MRI and CT, the difference between the cutoff points of these two methods was small [28]. In patients with GSDs, changes in the configuration and delayed ossification of the occipital condyles, cervical vertebrae and facet joints accentuate the mobility of the spine and alter CCJ parameter measurements on XR [8,26,33].

XR allows investigation of platybasia, basilar impression/invagination and atlantoaxial instability, and considering the agreement with CT, XR may complement MRI evaluations [26,27,34].

The basio dental interval measurements on CT were not in

agreement with the measurements obtained on XR and MRI, as demonstrated in other studies [22,35]. The worse performance of the atlanto-occipital interval assessment on MRI is probably due to the standardized protocol for evaluation of the cervical spine used in this study. Thus, CT is recommended when atlanto-occipital instability is suspected.

The measurements of the anteroposterior diameter of the spinal canal at C2 on CT were inferior to those on XR with good agreement and a high determination coefficient between XR and CT, indicating a constant bias related to the magnification caused by XR. Measurements of the same CCJ parameter on MRI were superior to those on CT, with lower agreement between MRI and CT, probably

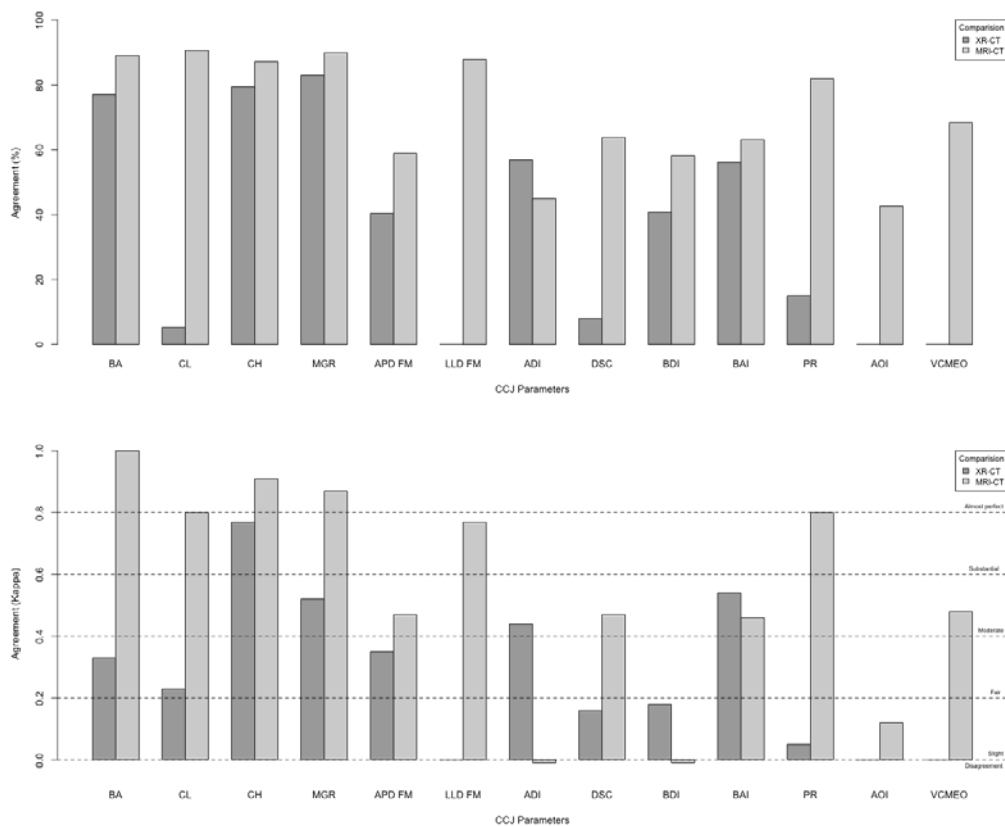


Figure 4: CCJ measurement reliability between XR-CT and MRI-CT by the Bland-Altman method (a) and by kappa statistics (b). CCJ: Craniocervical Junction; BA: Basal Angle; CL: Clivus Length; CH: Distance from the tip of the odontoid process to the Chamberlain Line; MGR: Distance from the tip of the odontoid process to the McGregor Line; APD: Anteroposterior Diameter; FM: Foramen Magnum; LLD: Latero-Lateral Diameter; ADI: Atlantodental Interval; DSC: Anteroposterior Diameter of the Spinal Canal; BDI: Basion-Dens Interval; BAI: Basion-Axial Interval; PR: Powers Ratio; AOI: Atlanto-Occipital Interval; VCME0: Ventral Cervicomedullary Encroachment by the Odontoid.

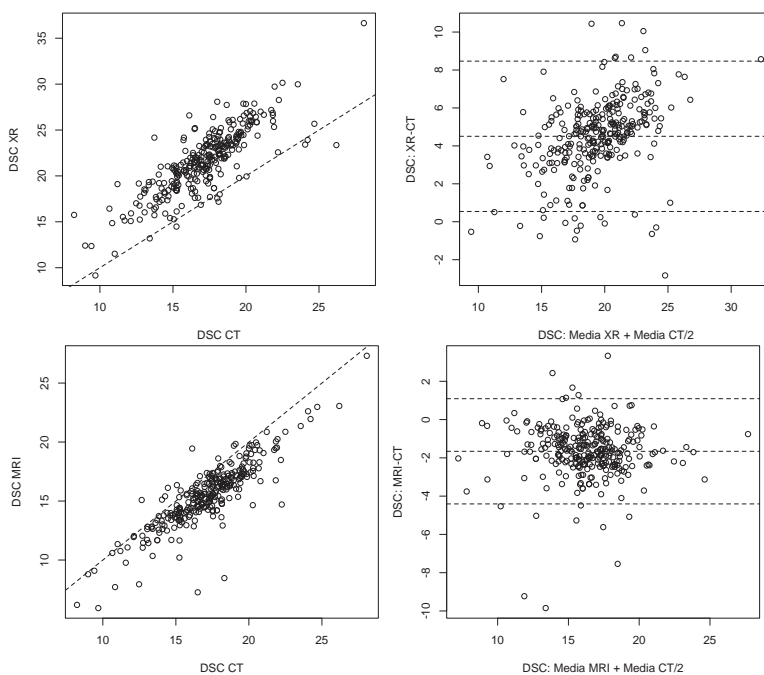


Figure 5: Correlation (a, c) and reliability (b, d) measurements of the diameter of the spinal canal (DSC) between XR-CT and MRI-CT by the Bland-Altman method.

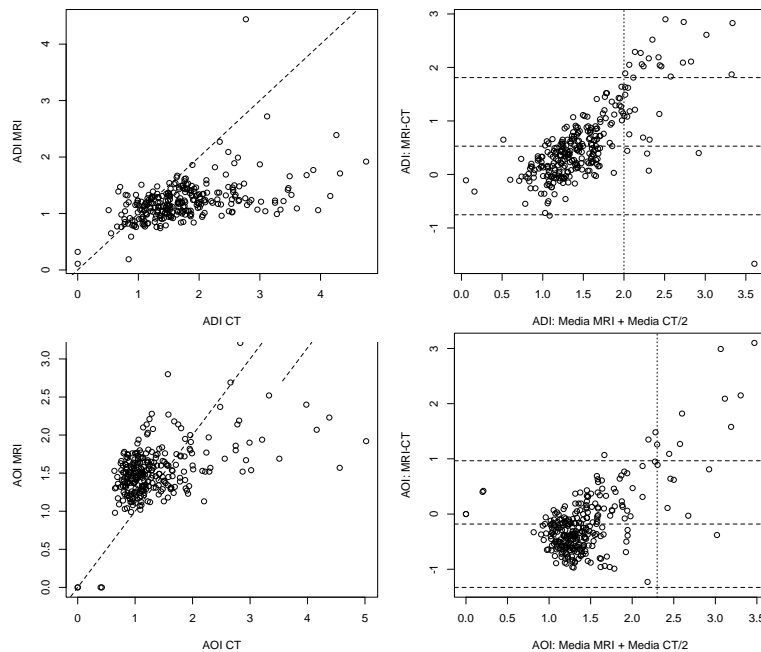


Figure 6: Correlation (a, c) and reliability (b, d) measurements of the Atlantodental Interval (ADI) on MRI-CT and the atlanto-occipital interval (AOI) on MRI-CT by the Bland-Altman method.

due to the enlargement of the image on XR and the difficulty of MRI in differentiating the cortical bone and ligaments.

The current study's limitations are as follows: the low frequency of CCJ changes and cSCI despite the significant sample size; a large number of patients with GSDs but a small number of patients with each type of GSD, limiting comparison of the risk between patients with different GSDs; a lack of inclusion of acute injuries considering that the referral center for rehabilitation treats patients with stable clinical conditions; the exclusion of children under four years of age, who would require sedation and its inherent risks; and the cross-sectional nature of the investigation, suggesting the need for further studies.

Craniovertebral junction imaging interpretation is difficult in patients with genetic skeletal disorders, and the possibility of spontaneous stabilization of the components should be considered as ossification of the axial skeleton occurs. XR and CT showed bone abnormalities. MRI showed cervical spinal cord injury. XR presented greater limitations but provided complementary data to MRI. CT showed the highest rates of interobserver and intraobserver agreement. Thus, XR, CT and MRI can be concluded to be complementary, and craniometry must be interpreted in conjunction with clinical data.

Summary Statement

Genetic skeletal disorders complicate the interpretation of craniocervical junction imaging. CT showed high reliability and should be performed when surgical treatment is indicated, or atlanto-occipital instability is suspected.

- CT showed the highest reproducibility and reliability for craniocervical junction parameters and is the best method for bone evaluation in patients with genetic skeletal diseases.

- XR exhibited more limitations for craniocervical measurements than CT and MRI; however, XR provided complementary data to MRI.

- Spinal canal stenosis at C2, a narrow foramen magnum, os odontoideum, ventral cervicomedullary encroachment by the odontoid, and basilar impression/invagination were associated with an increased chance of cervical spinal cord injury.

Acknowledgment

I would like to thank the Rede SARAH, the patients affected by genetic skeletal diseases and their relatives who made this study possible.

Funding

This research was supported by Rede SARAH.

References

1. Smoker WR, Khanna G. Imaging the craniocervical junction. *Child's Nervous System*. 2008; 24: 1123–1145.
2. Ji W, Kong GG, Zheng MH, Wang XY, Chen JT, Zhu QA. Computed tomographic morphometric analysis of pediatric clival screw placement at the craniovertebral junction. *Spine (Phila Pa 1976)*. 2015; 40: 259–265.
3. Hecht JT, Nelson FW, Butler IJ, Horton WA, Scott CI, Wassman ER, et al. Computerized tomography of the foramen magnum: Achondroplastic values compared to normal standards. *American Journal of Medical Genetics*. 1985; 20: 355–360.
4. Bertozzi JC, Rojas CA, Martinez CR. Evaluation of the pediatric craniocervical junction on MDCT. *AJR. American Journal of Roentgenology*. 2009; 192: 26–31.
5. Gholwe PA, Hosalkar HS, Ricchetti ET, Pollock AN, Dormans JP, Drummond DS. Occipitalization of the atlas in children. Morphologic classification, associations, and clinical relevance. *The Journal of Bone and Joint Surgery*. 2007; 89: 571–578.

6. Batista UC, Joaquim AF, Fernandes YB, Mathias RN, Ghizoni E, Tedeschi H. Computed tomography evaluation of the normal craniocervical junction craniometry in 100 asymptomatic patients. *Neurosurgical Focus*. 2015; 38: 5.
7. Chen YF, Liu HM. Imaging of craniovertebral junction. *Neuroimaging Clinics of North America*. 2009; 19: 483–510.
8. Deliganis AV, Baxter AB, Hanson JA, Fisher DJ, Cohen WA, Wilson AJ, et al. Radiologic spectrum of craniocervical distraction injuries. *Radiographics*. 2000; 20: 237–250.
9. Barbosa-Buck CO, Orioli IM, da Graça Dutra M, Lopez-Camelo J, Castilla EE, Cavalcanti DP. Clinical epidemiology of skeletal dysplasias in South America. *American Journal of Medical Genetics. Part A*. 2012; 158: 1038–1045.
10. Dominguez R, Talmachoff P, Rodriguez A. Radiological evaluation of the craniocervical junction in bone dysplasias and other related syndromes. *Clinical Imaging*. 1995; 19: 77–84.
11. Lachman RS. The cervical spine in the skeletal dysplasias and associated disorders. *Pediatric Radiology*. 1997; 27: 402–408.
12. Wynn J, King TM, Gambello MJ, Waller DK, Hecht JT. Mortality in achondroplasia study: A 42-year follow-up. *American Journal of Medical Genetics. Part A*. 2007; 143: 2502–2511.
13. Wagner MW, Poretti A, Benson JE, Huisman TA. Neuroimaging findings in pediatric genetic skeletal disorders: A review. *Journal of Neuroimaging*. 2017; 27: 162–209.
14. Hunter AG, Bankier A, Rogers JG, Sillence D, Scott CI. Medical complications of achondroplasia: A multicentre patient review. *Journal of Medical Genetics*. 1998; 35: 705–712.
15. ASIA and ISCoS International Standards Committee. The 2019 revision of the international standards for neurological classification of spinal cord injury (ISNCSCI)-what's new? *Spinal Cord*. 2019; 57: 815–817.
16. Panicker JN, de Sèze M, Fowler CJ. Rehabilitation in practice: Neurogenic lower urinary tract dysfunction and its management. *Clinical Rehabilitation*. 2010; 24: 579–589.
17. Helenius I, Crawford H, Sponseller PD, Odent T, Bernstein RM, Stans AA, et al. Rigid fixation improves outcomes of spinal fusion for C1-C2 instability in children with skeletal dysplasias. *The Journal of Bone and Joint Surgery*. 2015; 97: 232–240.
18. Pauli RM, Horton VK, Glinski LP, Reiser CA. Prospective assessment of risks for cervicomedullary-junction compression in infants with achondroplasia. *American Journal of Human Genetics*. 1995; 56: 732–744.
19. White KK, Bompadre V, Goldberg MJ, Bober MB, Campbell JW, Cho TJ, et al. Best practices in the evaluation and treatment of foramen magnum stenosis in achondroplasia during infancy. *American Journal of Medical Genetics*. 2016; 170: 42–51.
20. Mortier GR, Cohn DH, Cormier-Daire V, Hall C, Krakow D, Mundlos S, et al. Nosology and classification of genetic skeletal disorders: 2019 revision. *American Journal of Medical Genetics. Part A*. 2019; 179: 2393–2419.
21. Ulbrich EJ, Schraner C, Boesch C, Hodler J, Busato A, Anderson SE, et al. Normative MR cervical spinal canal dimensions. *Radiology*. 2013; 271: 172–182.
22. Martinez-Del-Campo E, Kalb S, Soriano-Baron H, Turner JD, Neal MT, Uschold T, et al. Computed tomography parameters for atlantooccipital dislocation in adult patients: The occipital condyle-C1 interval. *Journal of Neurosurgery. Spine*. 2016; 24: 535–545.
23. Landis JR, Koch GG. The measurement of observer agreement for categorical data. *Biometrics*. 1977; 33: 159–174.
24. Horton WA, Hall JG, Hecht JT. Achondroplasia. *Lancet*. 2007; 370: 162–172.
25. Morgan DF, Young RF. Spinal neurological complications of achondroplasia. Results of surgical treatment. *Journal of Neurosurgery*. 1980; 52: 463–472.
26. Copley LA, Dormans JP. Cervical spine disorders in infants and children. *The Journal of the American Academy of Orthopaedic Surgeons*. 1998; 6: 204–214.
27. Kornblum M, Stanitski DF. Spinal manifestations of skeletal dysplasias. *The Orthopedic Clinics of North America*. 1999; 30: 501–520.
28. Brühl K, Stoeter P, Wietek B, Schwarz M, Humpl T, Schumacher R, et al. Cerebral spinal fluid flow, venous drainage and spinal cord compression in achondroplastic children: Impact of magnetic resonance findings for decompressive surgery at the cranio-cervical junction. *European Journal of Pediatrics*. 2001; 160: 10–20.
29. Song D, Maher CO. Spinal disorders associated with skeletal dysplasias and syndromes. *Neurosurgery Clinics of North America*. 2007; 18: 499–514.
30. Ellingson BM, Woodworth DC, Leu K, Salamon N, Holly LT. Spinal cord perfusion MR imaging implicates both ischemia and hypoxia in the pathogenesis of cervical spondylosis. *World Neurosurgery*. 2019; 128: 773–781.
31. Rchette P, Bardin T, Stheneur C. Achondroplasia: From genotype to phenotype. *Joint Bone Spine*. 2008; 75: 125–130.
32. Vleggeert-Lankamp C, Peul W. Surgical decompression of thoracic spinal stenosis in achondroplasia: Indication and outcome. *Journal of Neurosurgery. Spine*. 2012; 17: 164–172.
33. Corcoran B, Linscott LL, Leach JL, Vadivelu S. Application of normative occipital condyle-C1 interval measurements to detect atlanto-occipital injury in children. *AJNR. American Journal of Neuroradiology*. 2016; 37: 958–962.
34. Solanki GA, Martin KW, Theroux MC, Lampe C, White KK, Shediak R, et al. Spinal involvement in mucopolysaccharidosis IVA (Morquio-Brailsford or Morquio A syndrome): Presentation, diagnosis and management. *Journal of Inherited Metabolic Disease*. 2013; 36: 339–355.
35. Li G, Passias P, Kozanek M, Shannon BD, Li G, Villamil F, et al. Interobserver reliability and intraobserver reproducibility of powers ratio for assessment of atlanto-occipital junction: Comparison of plain radiography and computed tomography. *European Spine Journal*. 2009; 18: 577–582.